

# We are IntechOpen, the world's leading publisher of Open Access books Built by scientists, for scientists

6,600

Open access books available

178,000

International authors and editors

195M

Downloads

Our authors are among the

154

Countries delivered to

TOP 1%

most cited scientists

12.2%

Contributors from top 500 universities



WEB OF SCIENCE™

Selection of our books indexed in the Book Citation Index  
in Web of Science™ Core Collection (BKCI)

Interested in publishing with us?  
Contact [book.department@intechopen.com](mailto:book.department@intechopen.com)

Numbers displayed above are based on latest data collected.  
For more information visit [www.intechopen.com](http://www.intechopen.com)



Chapter

# Adaptive Neuro-Fuzzy Inference System-Based GPS-IMU Data Correction for Capacitive Resistivity Underground Imaging with Towed Vehicle System

*Elmer Dadios, Jonah Jahara Baun, Mike Louie Enriquez, Adrian Genevie Janairo, Ronnie Concepcion II, Joseph Aristotle De Leon, Kate Francisco, Andres Philip Mayol, Argel Bandala and Ryan Rhay Vicerra*

## Abstract

This study proposes the utilization of an Adaptive Neuro-Fuzzy Inference System (ANFIS) to correct the latitude and longitude of Global Positioning System (GPS) used in locating towed vehicle system for underground imaging. The input used was the collected data from a developed Real-time Kinematic Global Positioning System sensor integrated with Inertial Measurement Unit. Different ANFIS models were developed and evaluated. For latitude correction, ANFIS model with hybrid optimization trained at 300 epochs was chosen, whereas for longitude correction, ANFIS model with hybrid optimization trained at 100 epochs was selected. Both models achieved the lowest Mean Squared Error (MSE), the highest Coefficient of Determination ( $R^2$ ), and lowest Mean Absolute Error (MAE). Moreover, selected best ANFIS models were compared to Long Short-Term Memory (LSTM) and Extreme Learning Machine (ELM) models, but the results showed that the ANFIS models have superior performances. The selected ANFIS models were verified by testing on the collected actual dataset and the visualized map demonstrated that the corrected GPS latitude and longitude have significantly reduced error, indicating that the fuzzy system with neural network capabilities is a cost-effective and convenient method for error reduction in vehicle localization making it applicable to be integrated for capacitive resistivity underground imaging systems.

**Keywords:** adaptive neuro-fuzzy inference, global positioning system, inertial measuring unit, underground imaging, towed vehicle

## 1. Introduction

Underground imaging is a noninvasive approach for creating a subsurface area model by transmitting low current, high alternating voltage, and low-frequency waves into the ground. This method has various applications such as detecting minerals, finding underground materials and faults, and detecting voids [1]. One of the techniques used in underground imaging is the capacitive resistivity (CR) method [1–3], where the ground-coupled transmitter and receiver antennas are designed and configured in a capacitive connection to measure resistivity by determining the potential difference [4–6]. The design of a capacitive resistivity imaging system can be either a single-pair antenna system that includes a transmitter and a receiver unit, or a multiple-antenna system with one transmitter and multiple receiver units [7]. Both systems use a vehicle towing mechanism during the surveying process, as presented in **Figure 1**, allowing for the mapping and location of buried utilities [8].

Accordingly, the CR method employs map-matching (MM) algorithms that utilize positioning sensors, such as the Global Positioning System (GPS) in combination with digital maps to determine the road link on which a vehicle is traveling and to obtain highly accurate data for mapping. GPS-based data collection is more efficient than traditional surveying and mapping approaches, requiring less equipment and labor [9]. It offers direct information on latitude and longitude coordinates without the need for angle and distance measurements between intermediary points. Despite its widespread use, GPS has some limitations that should be considered. For instance, GPS units cannot always provide locations with high accuracy beyond 3 meters, which could be problematic for certain applications. In addition, GPS devices rely on signals from at least four satellites to precisely pinpoint a location, and signal blocking or interference, such as in urban areas or under tree canopies, can impact performance. GPS accuracy may also be affected in environments with high ionospheric activity, such as during solar flares or geomagnetic storms. Finally, raw, uncorrected GPS data

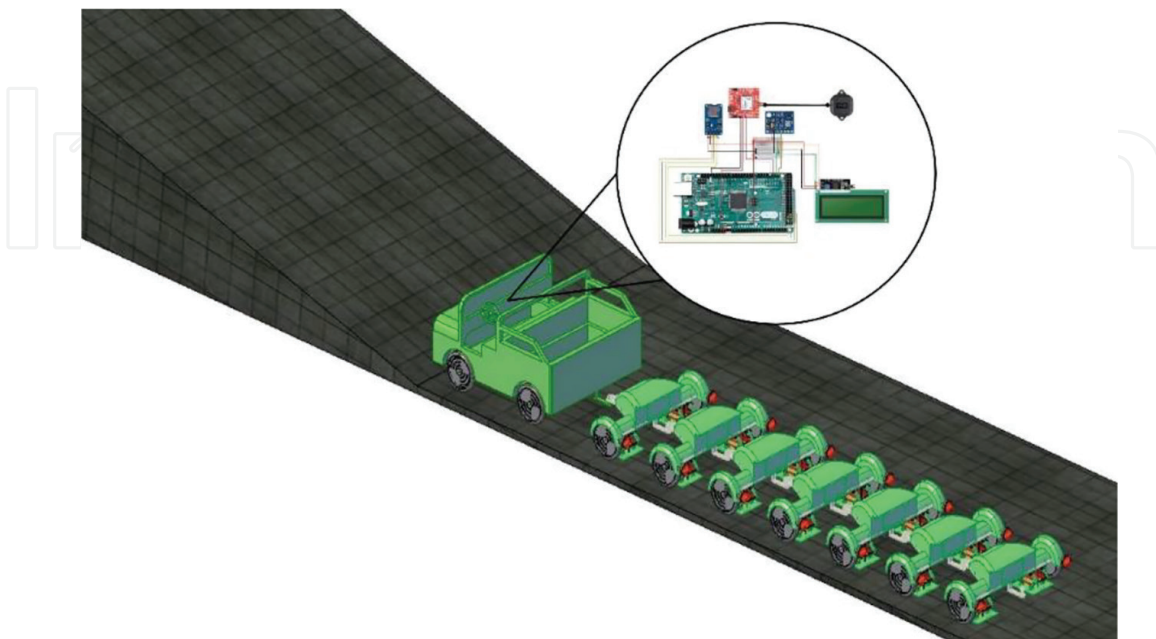


**Figure 1.**

*The placement of the GPS-IMU device utilized for localization and tracking of the capacitive resistivity towed antenna system used for underground imaging is illustrated.*

points may only be precise up to 5 meters, and a clear view of the sky is necessary to receive signals from GPS satellites [10, 11]. In capacitive resistivity imaging, lowering GPS accuracy error is critical for finding underground utilities and performing map matching, however, the mapping technology used in conjunction with GPS may not always be up-to-date or reliable, potentially leading to navigational errors [12, 13].

One known method to overcome the inaccuracy of mapping GPS sensor data alone is the IMU-GPS sensor fusion. This technique combines data from a GPS receiver and an Inertial Measurement Unit (IMU) to improve the accuracy and robustness of navigation and positioning systems [14]. It provides data regarding the orientation and acceleration of the device, while GPS provides information about its absolute position. By integrating the data from both sensors, the position and orientation estimates are more precise and reliable than the readings obtained from each sensor separately [14, 15].

In contrast to the state-of-the-art, which typically employs more conventional methods for localizing and land vehicle tracking, for instance, the Kalman filter, fuzzy logic is considered a commonly known artificial intelligence (AI) approach. Researchers in [16] created a strong Kalman filter utilizing vector tracking and integrated it with fuzzy logic to change filter parameters to follow weak signals in global navigation satellite system (GNSS) receivers. Thus, the results were superior to the standard procedure. Following this work, a fuzzy position correction method for latitude and longitude data from a GPS sensor was introduced, which was implemented on Field-Programmable Gate Arrays (FPGA) to speed up rectification results. Compared to other models, the FPGA-based approach provided a 40,000× speedup [17]. Combining antenna optimization techniques and sensor fusion with AI has been introduced to increase GPS accuracy [18]. Even when employing an inexpensive GPS sensor for location-based applications, this effectively computed correct latitude and longitude data. In another study, the authors utilized an unscented Kalman filter (UKF) and an unscented H-infinity (UH) filter to track ground vehicle position using fuzzy logic to decide which to use at any given time, lowering error by 5.6% and enhancing GPS accuracy [19]. Moreover, a fuzzy system model was developed [20] that flexibly adjusts the noisy covariance values of the extended Kalman filter (EKF) by combining data from GPS, an odometer, IMU, and the automobile's mathematical framework. This results in a 49% improvement in the precision of the vehicle's absolute position [20]. Similarly, Zhu et al. employed EKF to fuse data from a four-wheeled robot's GPS, IMU, odometers, and camera. They created a fuzzy system to adjust the noisy covariances of the EKF. The strategy successfully improves the robot's estimation of the trajectory to be followed by 80.6% [21]. These studies suggest that fuzzy logic has a great potential to be utilized for land vehicle tracking and localization, providing higher accuracy than the traditional approaches.

One type of artificial intelligence that integrates the capabilities and strengths of both neural networks and fuzzy logic systems is the adaptive neuro-fuzzy inference system (ANFIS), which is used for analyzing input–output relations, can handle inaccurate or imperfect data and has been useful to various domains such as in pattern recognition and predictive modeling [22]. Specifically, ANFIS has also been employed in the localization and tracking of land vehicles and shows significant findings in different scenarios. The work in [23] classified direct, multipath-affected, and non-line of sight (NLOS) findings using raw GPS measurements with an ANFIS algorithm. The correct classification rates were 100, 91, and 84%, respectively. Another study proposed an intelligent ANFIS system that modifies the position of a vehicle based on sensor data and latitude/longitude. According to the results, the fuzzy system outperformed the unscented Kalman filter by 69.2% [24]. Another study employs ANFIS to estimate an

IMU's inaccuracy over time. While it refrains from specifically addressing GPS-IMU incorporation, it offers details on the application of ANFIS for IMU data error estimation, and the outcome implies that the ANFIS could substantially enhance the accuracy of inertial navigation positioning, which is important for vehicle inertial navigation in intricate and covert settings [25]. Research by [26] presents an ANFIS-based approach to categorizing everyday life events using data collected by IMU sensors. Although it concentrates on identifying activities rather than GPS-IMU data correction, it still exhibits the usage of ANFIS in sensor fusion with a total accuracy of 98.88%. The real-time deployment of ANFIS for vehicle navigation is proposed in [27]. When evaluated on a vehicle, the suggested model outperforms standard methods in terms of accuracy. The experimental findings proved the benefits of the suggested AI-based INS/GPS integration strategies in terms of robustness while maintaining real-time system location accuracy [27]. Although ANFIS has several advantages for GPS-IMU localization and vehicle tracking, it is vital to evaluate the potential limits and challenges of employing this technology. In [24, 28], the study showed that one potential limitation of ANFIS is that it may necessitate a huge amount of data to accurately train the model, and ANFIS models can be complex and hard to understand, which renders it more challenging to comprehend how the model works and makes decisions, particularly for autonomous vehicle applications. Thus, future research still requires more exploration of ANFIS modeling to prove its advantages and disadvantages in certain fields.

In relation to this proposed study, the main objective is to correct the GPS sensor's latitude and longitude coordinates to avoid complex mathematical operations and achieve a comprehensive location system embedded in a towed antenna system. Thus, it is critical to reduce the error in the accuracy of GPS receivers, which ensures the correct location of underground utilities and for map matching purposes. With that, this study aims to propose an intelligent system-based fuzzy logic using ANFIS, which takes the information from Real-time Kinematics (RTK) GPS sensors with integrated IMU's linear acceleration and orientation data, which corrects the capacitive resistivity imaging system vehicle's absolute position according to its latitude and longitude. This correction uses two fuzzy systems, one for latitude and the other for longitude, which will be trained using the ANFIS tool. The positioning correction system will be trained and tested with datasets from constructed Arduino-based RTK-GPS with Integrated IMU. Moreover, the developed models are compared to the performance of two neural network models – long short-term memory (LSTM) and extreme learning machine (ELM) for the comparison and validation of the proposed method. This research is expected to provide significant benefits, including (1) facilitating the integration of different measurement modalities and improving the interpretation and visualization of the data [29] which can enhance the understanding of the subsurface properties being investigated in capacitive resistivity imaging (CRI) systems, (2) aid in mapping the precise location of the underground utility objects being surveyed by the underground imaging towed antenna system, and (3) the ability to automate data acquisition and processing, which can save time and reduce errors and provide more precise control over the measurement process, enabling more accurate and reproducible results.

## **2. Materials and methods**

The proposed step-by-step procedures of how to correct the collected GPS sensor's latitude and longitude coordinates used to find the position of the towed array vehicle in an underground imaging system are presented in **Figure 2**. This provides a

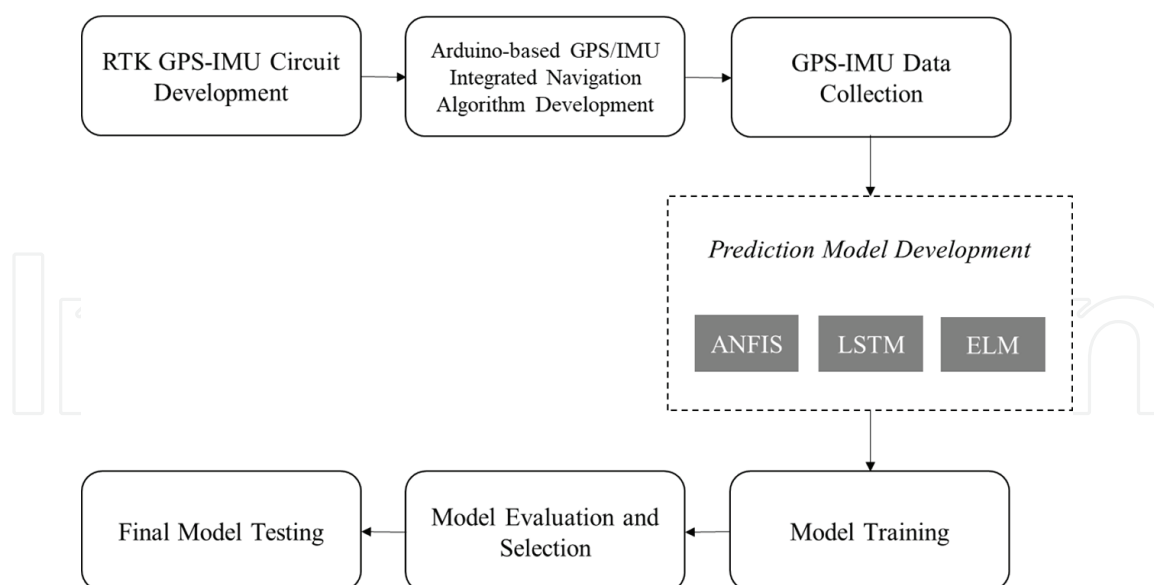


**Figure 2.** Step-by-step process of GPS sensor's latitude and longitude coordinates correction used for the capacitive resistivity underground imaging system.

functional view of how the whole research system works. The process starts with the hardware circuit development of an RTK-GPS sensor with an integrated IMU sensor, followed by the incorporation of a developed Arduino-based GPS/IMU integrated navigation algorithm to complete the device needed for GPS and IMU data collection, which is conducted through actual field testing. After collecting the data, three prediction models were developed: ANFIS, LSTM, and ELM, while the collected data were trained using these three models to predict the corrected GPS latitude and longitude. The prediction model with the highest accuracy was selected while LSTM and ELM prediction models were also used to validate the performance of ANFIS and, thus, utilized for final model testing of collected data.

## 2.1 Arduino-based RTK-GPS with integrated IMU

An Arduino-based RTK-GPS with an integrated IMU is a device that combines a real-time kinematic (RTK) global positioning system (GPS) with an inertial measurement unit (IMU) using an Arduino microcontroller. The overall block diagram of how the RTK-GPS is combined with the IMU sensor is presented (**Figure 3**) to comprehend the overall system architecture and information flow between various functional parts. The RTK-GPS utilized is a Sparkfun SMA-ZED-F9P model, which is the highest-quality module for high-accuracy GNSS and GPS navigation solutions, including RTK, with 10 mm three-dimensional accuracy, while the utilized IMU sensor is GY-85 9DOF Sensor that has nine axes which are triaxial gyroscope, triaxial accelerometer, and triaxial magnetic field. The RTK-GPS sensor can calculate the satellite position and velocity and provides a GPS raw pseudo-range that is the pseudo-distance between the satellite and GPS receiver, and the pseudo-rate specifies the velocity. Through this, the RTK-GPS sensor strengthens GPS signals for exact locations and velocities. On the other hand, the IMU sensor performs the coordination rotation, which is the process of aligning the axes of the IMU sensor with the axes of the vehicle where it is mounted. It also performs altitude determination. These two are significant aspects of sensor fusion in localization and vehicle tracking. Then, by

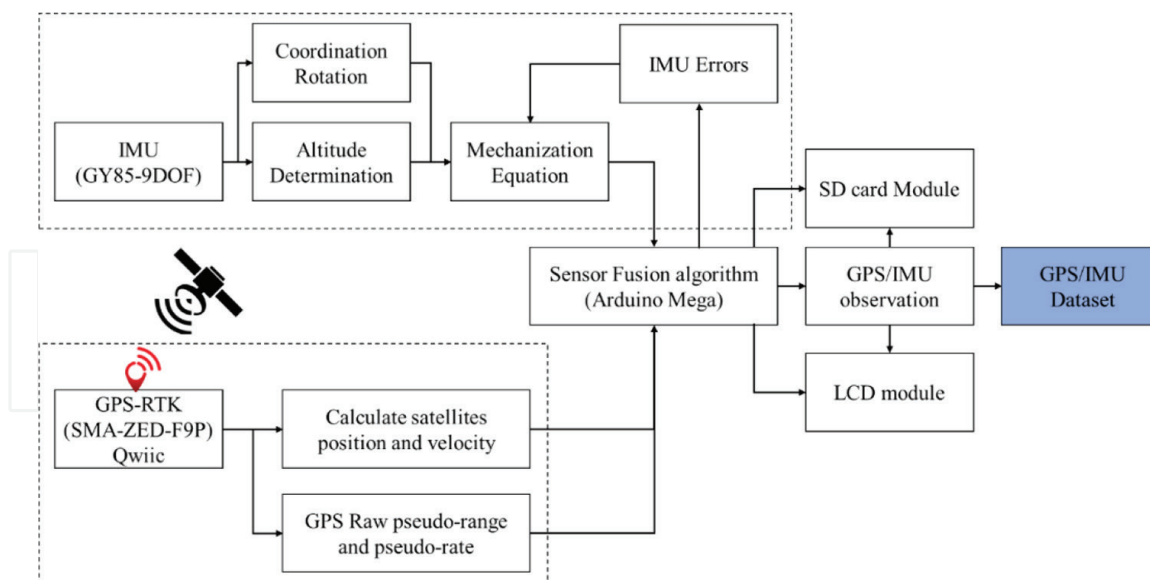


**Figure 3.**

*Block diagram of the development of Arduino-based GPS-RTK with integrated IMU for sensor fusion.*

utilizing mechanization equations, the accelerometer, gyroscope, and magnetometer in the IMU sensor module offer information on linear acceleration, angular velocity, and magnetic field strength along three axes, also considering the estimation errors present in the computation process. If IMU errors are not dealt with or assessed correctly as part of a combined GPS-IMU system, these can cause major inaccuracies in location, velocity, and attitude calculation. To build the system, the RTK-GPS sensor, IMU sensor, Secure Digital (SD) card module, and LCD monitor are connected to the Arduino mega board using various interfaces such as serial peripheral interface (SPI), inter-integrated circuit (I2C), and universal asynchronous receiver/transmitter (UART). Once the components are connected, necessary libraries [30] are installed, and the algorithm for sensor fusion is written to read data from the RTK-GPS and IMU, store the data on the Secure Digital (SD) card, and display the data on the LCD monitor in real-time. Thus, providing an output of the GPS-IMU dataset.

To show the actual electrical connections between the components in the circuit, the electronic circuit diagram is presented (**Figure 4**) to create a powerful system that can provide high-precision positioning data and information about the device's orientation and movement.

Overall, the RTK-GPS component provides high-precision positioning data [31, 32], while the IMU [32–34] component provides information about the device's orientation and movement. Combining these two components can produce more accurate and reliable data than either component alone. By combining the functionalities of the RTK-GPS and IMU, the device provides more accurate and reliable data than either component alone [34]. As a result, it is a vital tool for a broad spectrum of applications requiring precise location and movement data. The setup function initializes the modules, sets the output rate of the RTK-GPS module to 20 Hz, creates a log file on the SD card, and initializes the  $20 \times 4$  LCD. The loop function reads data from the RTK-GPS module, converts it into a more readable format, and writes it to the log file and LCD display. The data logged includes the latitude, longitude, mean sea level and accuracy. In addition, the code was designed to read data from the IMU sensor module, which contains an accelerometer, a magnetometer, and a gyroscope. The data includes acceleration, magnetic field strength, and angular velocity in three axes, as well as gyroscope temperature.

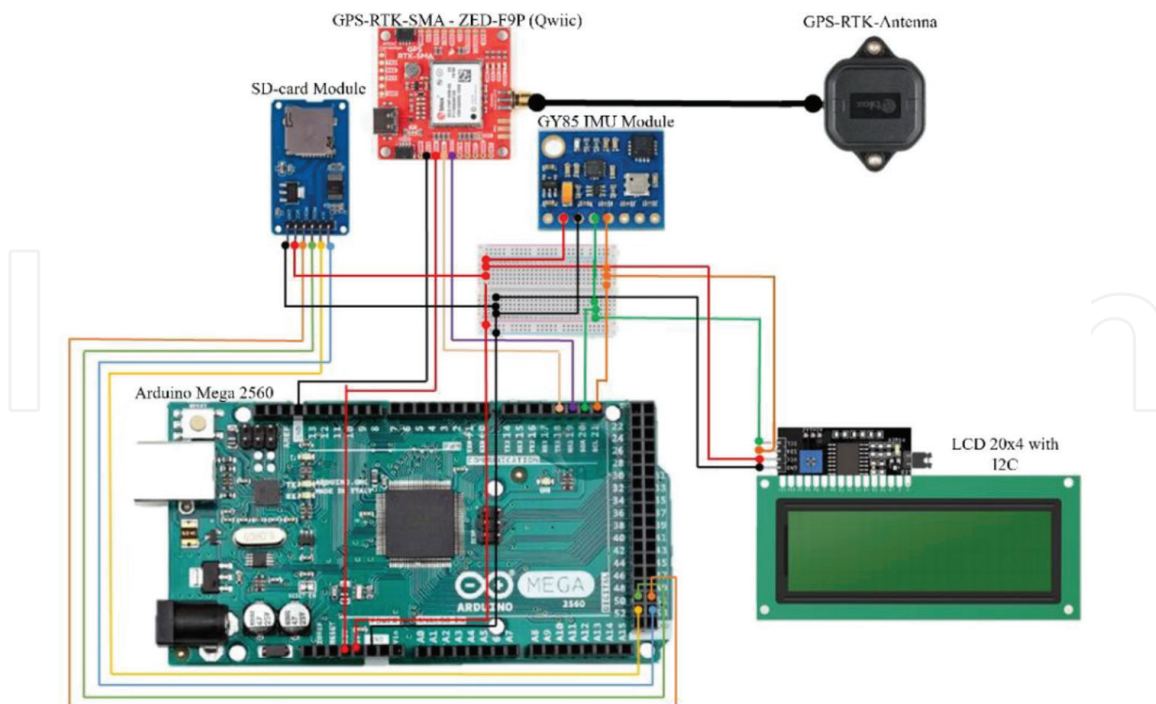


**Figure 4.**  
*Circuit diagram of Arduino-based GPS-RTK with integrated inertial measurement unit.*

## 2.2 Integrated GPS-IMU data collection

Using the Arduino-based integrated GPS-IMU device with sensor fusion algorithm, a total of 2521 row data of GPS latitude and longitude, triaxial accelerometer, and triaxial magnetometer information were collected. The device was mounted in front of a testing vehicle while the circuit testing was conducted, starting from a specific point at Lumban, Laguna, and ending at De La Salle University (DLSU) Manila Campus.

The data from RTK-GPS with an integrated IMU sensor is acquired and logged through the connected SD card in the Arduino, and it automatically saves all the collected data in Comma Separated Values (CSV) files to be able to present the data in tabular format and efficient data processing. To verify if the collected actual data has significant errors, the collected GPS latitude and longitude data from the testing route were plotted into a map, as seen in **Figure 5** (in red pin markers). The plotting of GPS latitude and longitude coordinates started by converting the saved CSV file into GPS eXchange Format (GPX) to properly store, exchange, and map GPS location data. MyGeodata Cloud is used in the conversion; this is an online converter tool that allows users to convert CSV files to GPX format in batch. Using Google Maps, the GPX file containing the collected GPS latitude and longitude is imported, and the map waypoints are automatically added and plotted. For the reference GPS points of latitude and longitude, the reference route is extracted from Google Maps and then converted to a GPX file. This GPX file is also plotted in Google Maps, as seen in **Figure 5** (the blue line), for comparison and visualization. The collected reference GPS latitude and longitude data were also utilized as the target output for the prediction models. Thus, **Figure 5** clearly represents the reference GPS data in the blue line and the plotted collected GPS data in red pin markers. From **Figure 6**, it is evident that the collected GPS data are not close to the reference route (blue line), which shows that there are inconsistencies and errors with the collected GPS data. The error is too large, which should be corrected using the ANFIS tool.



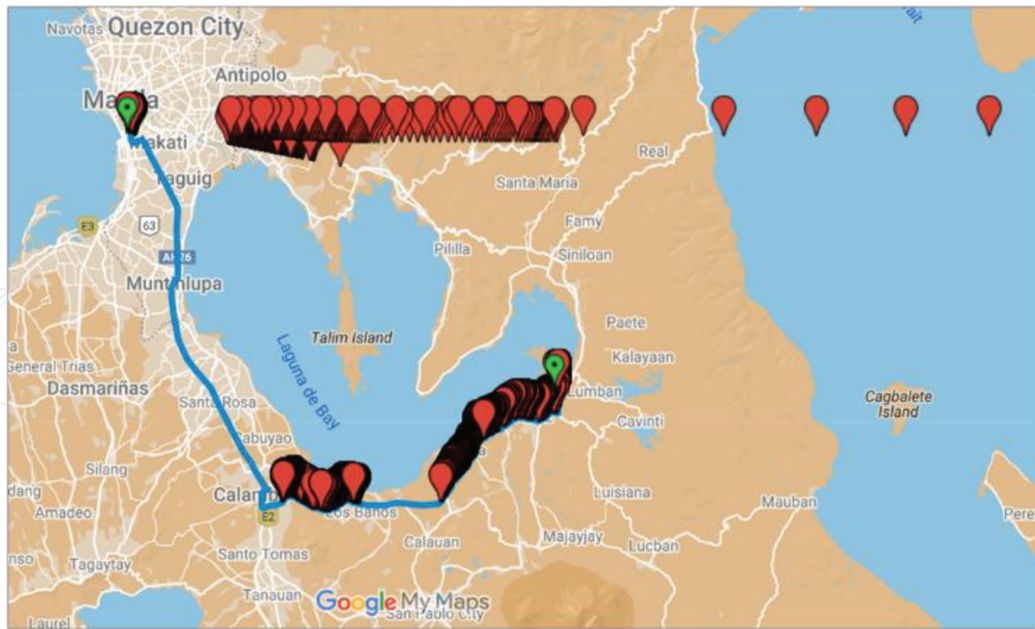


**Figure 5.** Mapped collected GPS data points (red pin markers) and reference route (blue line) from Lumban, Laguna to DLSU.

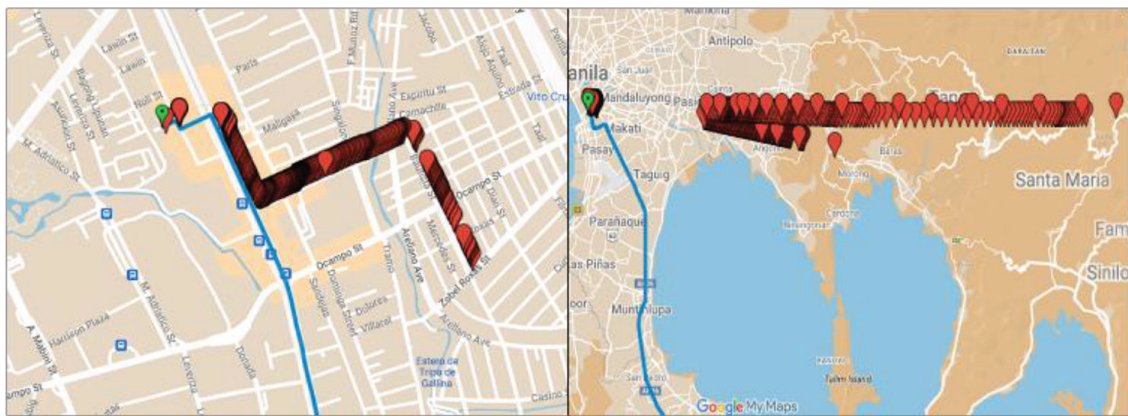


**Figure 6.** Inconsistencies and errors of collected GPS data (red pin markers) with respect to the reference route (blue line).

### 2.3 Adaptive neuro-fuzzy inference system modeling

ANFIS, an Adaptive Neuro-Fuzzy Inference System, is an intelligent system that combines the capabilities of Artificial Neural Network (ANN) and Fuzzy Logic Inference System (FIS) to bridge the gap that exists between the two [35–37]. This is a well-established technique that employs relational models to represent linear and nonlinear relationships between input and output parameters, taking into account the fact that human knowledge is often fuzzy and not strictly defined [35]. The function of the human nervous system is depicted by the Fuzzy Inference System (FIS), which is supported by the Artificial Neural Network (ANN). A neuro-fuzzy component forms each layer of the ANFIS, which can be recognized as a feedforward ANN that was developed by [36]. The input variables' activation process will take place via the function parameters, which are trained using an optimization method defined by the input membership function (MF) and then passed on to the next neuron. Following

this, the activation values will be identified by the fuzzy rules and sent to the output MF before being transferred to the output node [35].

Through ANFIS, a fuzzy system may correct several inputs at the same time, and these multiple inputs employed in the ANFIS model are GPS latitude, GPS longitude, 3-axis point coordinates of the accelerometer, and 3-axis point coordinates of the magnetometer. Two fuzzy systems are developed in this case, one for correcting the latitude and the other for longitude correction. The combined GPS and IMU sensors provided the same data to both fuzzy systems. The data used for training and testing are collected data through the GPS-RTK with an integrated IMU sensor. In particular, the subclustering method was utilized for FIS generation in the two models-latitude and longitude, as it demonstrated the best performance during algorithm pre-evaluation. This method generates a Sugeno-type FIS structure that is utilized to initialize the membership function parameters (Figures 7 and 8) [38]. This method involves dividing the input space into several subsets, known as clusters, and identifying the optimal number of clusters required to represent the input space accurately [39]. Once the clusters are identified, the corresponding membership function parameters are initialized based on the cluster centers and widths. This initialization allows for faster and more accurate training of the ANFIS network using two different optimization methods.

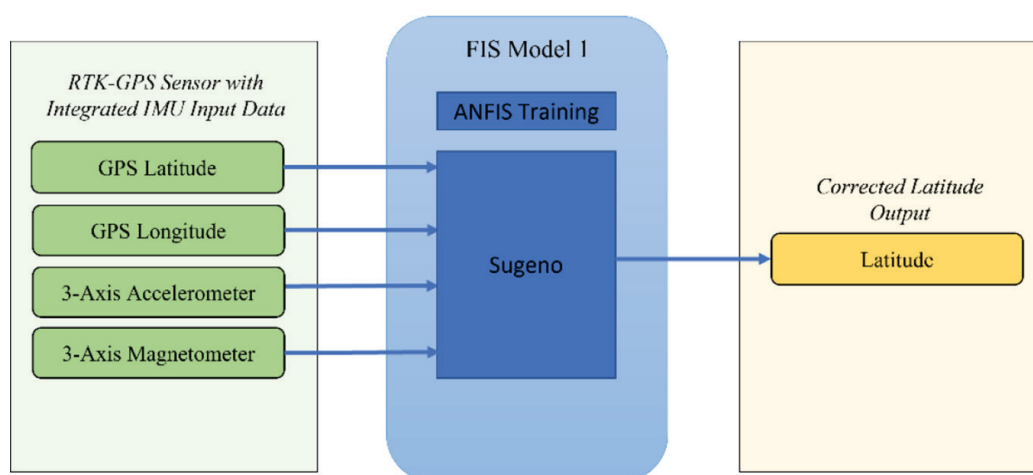


**Figure 7.**  
*Sugeno-type FIS for training the latitude ANFIS model.*

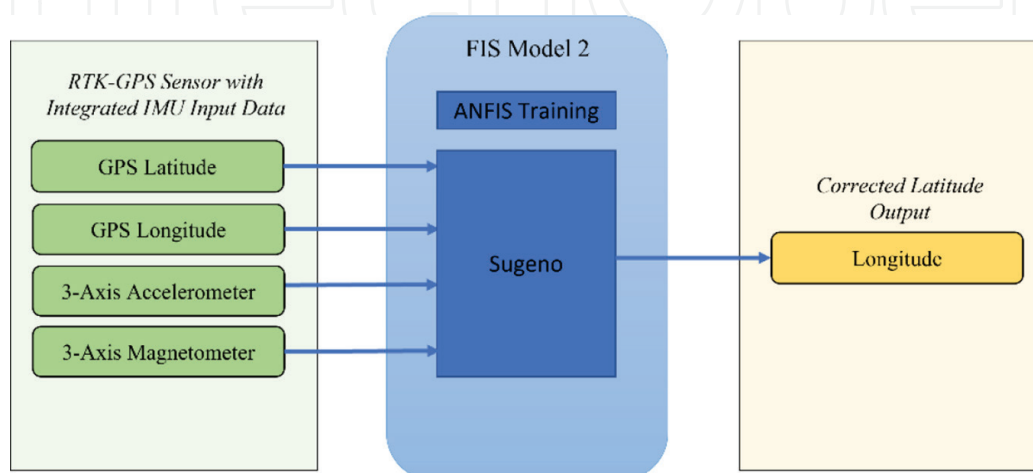


**Figure 8.**  
*Sugeno-type FIS for training the longitude ANFIS model.*

In the ANFIS tool, the range of influence was configured to 0.25 to allow the model to create smaller data clusters and produce more fuzzy rules. The squash factor is 0.6 to also create more and smaller data clusters. The acceptance ratio value is 0.25, which is greater than the rejection ratio value of 0.15. For each of the two models, four models are generated by changing the number of epochs of either 100 or 300 and altering the optimization methods used-hybrid, which is the combination of back-propagation and least mean squared error method and backpropagation. The best model will be selected based on which has the lowest error in training and testing.

For the latitude correction ANFIS model (**Figure 9**), the resulting ANFIS structure has eight inputs and one output node with 21 input MF for each input, generating 21 fuzzy rules and 389 nodes. The eight inputs represent the collected GPS latitude and longitude data points, the 3-axis coordinates of the accelerometer, the 3-axis coordinates of the magnetometer, and the reference latitude as the targeted output. The rest of the other latitude models followed the same structure and configuration of the network.

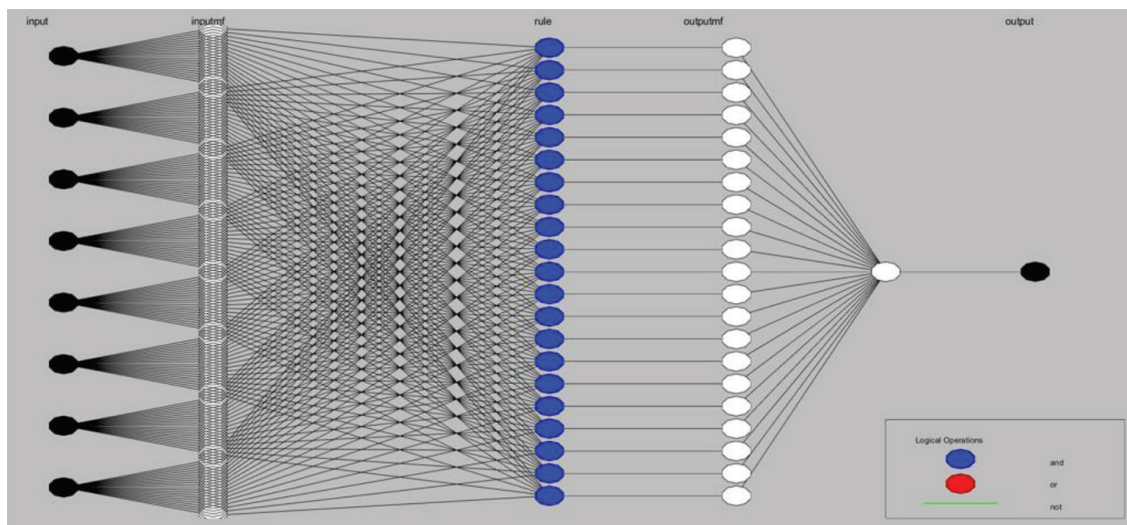


**Figure 9.**  
ANFIS subclustering network structure for corrected latitude prediction.

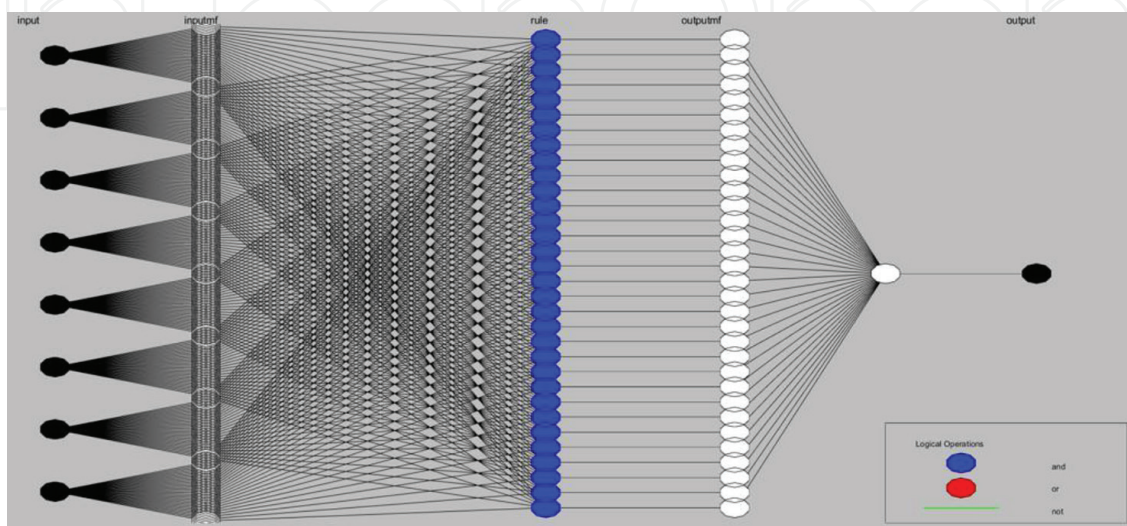


**Figure 10.**  
ANFIS subclustering network structure for corrected longitude prediction.

Moreover, **Figure 10** shows the resulting ANFIS structure of the longitude correction ANFIS model that has eight inputs-the collected GPS latitude and longitude datapoints, 3-axis coordinates of the accelerometer, and 3-axis coordinates of the magnetometer, and reference longitude as the target output with 32 input MF for each input allowing to producing of 32 fuzzy rules and 439 nodes. All the simulated longitude models followed the same structure and configuration of the network.

## 2.4 Long short-term memory (LSTM) and extreme learning machine (ELM) modeling

A special kind of Recurrent Neural Network that can recognize long-term dependencies is known as Long Short-Term Memory Network or LSTM. LSTMs are designed specifically to avoid the long-term dependence problem [40]. Their behavior is set up to make retention of memory over time their default setting. Therefore, they perfectly compare time series forecasting [40]. This study employs LSTM to develop prediction models for latitude and longitude correction. The hyperparameters used in modeling are presented in **Table 1**. A three-layer LSTM network was simulated with different combinations of hidden neurons on each layer. Hidden layer 1 comprises 500, 1000, and 1500 hidden neurons; hidden layer 2 has 700, 500, and 300 hidden neurons, while hidden layer 3 shall consist of 300, 200, and 100 hidden neurons. These different combinations of hidden neurons were modeled with three various training epochs of 100, 200, and 300 to generate several combinations of LSTM prediction networks. Moreover, the training optimizer used is “sgdm” or the Stochastic Gradient Descent with momentum with a set initial learning rate of 0.001, a mini-batch size of 128 to learn the common patterns as important features, and a gradient threshold of 1.

On the other hand, Extreme Learning Machine or ELM is also applied to generate prediction models. ELMs are feedforward neural networks having one or more layers of hidden nodes that are used to analyze data and predict values [41]. These hidden nodes’ parameters require no adjustment for selecting features, compression, clustering, classification, or sparse estimation [41]. To ensure lower error rates, weights to these concealed nodes may be assigned using the stochastic projection method, or these nodes can be passed down from their predecessors and not changed. In contrast to conventional gradient-based methods of learning for feedforward neural networks, ELM offers intriguing and important characteristics [42]. In comparison to

Hyperparameters	Value
Number of Hidden Neurons in Layer 1	500, 1000, 1500
Number of Hidden Neurons in Layer2	700, 500, 300
Number of Hidden Neurons in Layer 3	300, 200, 100
Number of Epochs	100, 200, 300
Training Optimizer	“sgdm”
Initial Learning Rate	0.001
Mini-Batch size	128
Gradient Threshold	1

**Table 1.**  
*Hyperparameters used in LSTM prediction modeling of latitude and longitude.*

Hyperparameters	Value
Number of Hidden Neurons	100, 200, 300, 400, 500, 600, 700, 800, 900, 1000
Activation Function	“radbas”

**Table 2.**  
*Hyperparameters used in ELM prediction modeling of latitude and longitude.*

gradient-based learning, ELM learning progresses far more quickly and performs well in generalization [43]. The hyperparameters used in the simulation of ELM models for latitude and longitude prediction are summarized in **Table 2**. A single-layer ELM is used, thus producing various models by simulating the different numbers of hidden neurons, which are given as 100, 200, 300, 400, 500, 600, 700, 800, 900, and 1000 while the selected activation function applied is the “radbas” or the radial basis function for good generalization and fast training.

### 2.5 Evaluation metrics for prediction model performance

The performance of the developed prediction models for latitude and longitude correction was evaluated using mean square error (MSE), root mean square error (RMSE), coefficient of determination ( $R^2$ ), and mean absolute error (MAE).

MSE calculates the average difference of squares between predicted and true values. MSE is used to assess the model’s quality based on predictions made across the entire training dataset versus the true label/output value. Lower MSE values suggest that the model is more accurate, and this is defined mathematically by (1):

$$MSE = \frac{1}{n} \sum_{i=1}^n \left( \hat{y}_i - y_i \right)^2 \quad (1)$$

The average difference between expected and actual values in a dataset is measured using the root mean square error (RMSE). The RMSE measures how distributed the residuals are, showing how closely the observed data clusters around the predicted values. Mathematically, RMSE is calculated as the square root of the MSE.

The coefficient of determination ( $R^2$ ) is a measure of how well the values fit in comparison to the original values. It calculates the percentage of the total variation in the variable that is dependent which can be explained by the model’s independent variables. The value is obtained as a percentage and ranges from 0 to 1. The greater the value, the better the model. It is calculated using (2).

$$R^2 = 1 - \frac{\sum_{i=1}^n \left( y_i - \hat{y}_i \right)^2}{\sum_{i=1}^n \left( y_i - \bar{y}_i \right)^2} \quad (2)$$

Finally, MAE indicates the difference between the true and predicted values, which is calculated by averaging the absolute difference over a given data set. It is typically utilized when measuring performance using continuous variable data.

It returns a linear number that equalizes the weighted individual differences. The smaller the value, the greater the performance of the model. It is computed using (3).

$$MAE = \frac{\sum_{i=1}^n |y_i - \hat{y}_i|}{n} \quad (3)$$

where  $n$  is equal to the number of data points,  $y_i$  is the observed values, and  $\hat{y}_i$  is the predicted values.

### 3. Results and discussion

#### 3.1 Analysis of results of ANFIS-based GPS-IMU data correction models

Different combinations of ANFIS optimization algorithms and several epochs are applied to train and test the data to select the best ANFIS model for GPS latitude and longitude correction. The 2521 input and output data rows were divided into training, validation, and test data. About 55% is used as training data, 25% for validation, and 20% for testing. The input data used are collected actual data, specifically the GPS latitude and longitude coordinates, 3-axis coordinates of the accelerometer, and 3-axis coordinates of the magnetometer, while the output data used is the extracted reference GPS latitude and longitude from Google Maps. The simulated models are further quantified numerically using training RMSE, validation RMSE, and testing RMSE. Presented in **Table 3** is the summary of simulated ANFIS models with different hyperparameters for latitude correction. Model 1 corresponds to the ANFIS latitude correction model, which resulted in four models known as models 1A, 1B, 1C, and 1D. In model 1A, hybrid optimization is applied, and after 100 epochs, the model training has stopped attaining training RMSE of 0.009121, validation RMSE of 0.008567, and testing RMSE of 0.012093. On the other hand, model 1C with the backpropagation algorithm applied was trained for 100 epochs, achieving training RMSE of 1.101670, validation MSE of 1.136290, and testing RMSE of 4.383700. Similarly, model 1D with the backpropagation algorithm at 300 epochs obtained a low training RMSE of 1.090430, validation RMSE of 1.114220, and testing RMSE of 4.473100. However, model 1B with a hybrid optimization algorithm achieved the lowest training RMSE of 0.008770, 0.008300 validation RMSE, and 0.011814 testing RMSE at 300 training epochs. It is evident that model 1B significantly exhibited the best training and test results out of the other models for GPS latitude correction using the simulated ANFIS tool.

Model 1	Optimization Algorithm	Epochs	Training RMSE	Validation RMSE	Testing RMSE
1A	Hybrid	100	0.009121	0.008567	0.012093
1B	Hybrid	300	0.008770	0.008300	0.011814
1C	Backpropagation	100	1.101670	1.136290	4.383700
1D	Backpropagation	300	1.090430	1.114220	4.473100

**Table 3.** Summary of simulated ANFIS models with different hyperparameters for latitude correction.

Model 2	Optimization Algorithm	Epochs	Training RMSE	Validation RMSE	Testing RMSE
2A	Hybrid	100	0.007361	0.007100	0.015321
2B	Hybrid	300	0.007361	0.007100	0.015321
2C	Backpropagation	100	0.766548	0.773640	3.360600
2D	Backpropagation	300	0.915090	0.905851	2.565400

**Table 4.** Summary of simulated ANFIS models with different hyperparameters for longitude correction.

Moreover, the summary of simulated ANFIS models for different combinations of hyperparameters for GPS longitude correction is presented in **Table 4**. In contrast to model 1, model 2 represents the ANFIS longitude correction model, which resulted in models 2A, 2B, 2C, and 2D models. Model 2C with the backpropagation algorithm applied was trained for 100 epochs, achieving a high training RMSE of 0.766548, validation MSE of 0.773640, and testing RMSE of 3.360600. But model 2D with a backpropagation algorithm at 300 epochs obtained the highest training RMSE of 0.915090, validation RMSE of 0.905851, and testing RMSE of 2.565400. With a hybrid optimization algorithm applied, model 1A and model 2B resulted in the lowest and same values of training RMSE, validation RMSE, and testing RMSE of 0.007361, 0.007100, and 0.015321, respectively. However, based on the training results, model 2B seems to overfit the training data and has a more complex model with higher computational resources required for training because of the higher training epoch value. Thus, the superior performance of model 2A in correcting GPS longitude is apparent as it has shown significantly better training and test results than the other models.

### 3.2 Analysis of results of GPS-IMU data correction models using LSTM and ELM

To compare and validate the results of the simulated ANFIS models, different LSTM and ELM models were also simulated to achieve their best-offered models. The 2521 input and output data rows were split into training, validation, and test data, as with ANFIS models. About 55% of the data is used for training, 25% for validation, and 20% for testing. The input data consists of actual data, particularly GPS latitude and longitude coordinates, accelerometer 3-axis coordinates, and magnetometer 3-axis coordinates. In contrast, the output data is the extracted reference GPS latitude and longitude from Google Maps. The simulations of LSTM models for latitude and longitude prediction were done in MATLAB. A total of nine combinations of LSTM networks using the different set hyperparameters have been modeled. From the different combinations, the results of the best combinations of the LSTM model are shown in **Table 5**. The table shows that an LSTM network comprised of 1500–700–300 hidden neurons for each of the three hidden layers with 300 epochs is the best

Parameter	LSTM Network	Epochs	Training RMSE	Validation RMSE	Testing RMSE
Latitude	1500–700–300	300	0.106777	0.100347	0.101889
Longitude	1500–700–300	200	0.145039	0.149588	0.149149

**Table 5.** Results of best LSTM models for latitude and longitude correction.

Parameter	ELM Hidden Neuron	Training RMSE	Validation RMSE	Testing RMSE
Latitude	100	0.072205	0.078897	0.079802
Longitude	100	0.109437	0.119175	0.138129

**Table 6.**

Results of best ELM models for latitude and longitude correction.

model for latitude correction among the other simulated models. This model obtained the least training RMSE of 0.106777, validation RMSE of 0.100347, and testing RMSE of 0.101889. Moreover, the best simulated LSTM model for longitude correction is the combination of 1500–700–300 hidden neurons for each of the three hidden layers with less training epochs of 200. Thus, this selected model obtained the least training RMSE of 0.145039, validation RMSE of 0.149588, and testing RMSE of 0.149149.

Compared to the LSTM models, **Table 6** also provides the results of the highest-performing simulated ELM models for latitude and longitude correction. From the results, the ELM network with 100 hidden neurons indicates the least training, validation, and testing RMSE for latitude and longitude correction. The training RMSE of the selected highest-performing ELM model for latitude correction is 0.72205, the validation RMSE is 0.78897, and its testing RMSE is 0.79802. On the other hand, the training RMSE of the highest-performing ELM model for longitude prediction is 0.109437, with a validation RMSE of 0.119175 and training RMSE of 0.138129.

### 3.3 Comparison of results between ANFIS, LSTM, and ELM

Using 25% of the collected data as validation data for model evaluation, the selected best ANFIS model performance is compared to the selected highest-performing LSTM and ELM models for latitude correction which is presented in **Table 7**. In terms of MSE, the selected best ANFIS model, model 1B from **Table 3**, showed significantly superior results compared to the LSTM and ELM models, which is 0.000069. Other evaluation metrics such as the  $R^2$  and MAE of 0.995479 and 0.000375, respectively, also signify that the best ANFIS model still offers superior performance.

Furthermore, among the simulated highest-performing ANFIS, LSTM, and ELM prediction models for longitude correction in **Table 8**, the ANFIS model, which is model 2A from **Table 4**, still has the most superior performance with attained MSE,  $R^2$ , and MAE of 0.000050, 0.997675, and 0.000042, respectively.

A scatter plot is presented to visualize the performance of the ANFIS models using the validation data (**Figures 11 and 12**) to compare further the relationship between the reference latitude/longitude and the predicted corrected latitude/longitude. The given plot is clear and concise, indicating a strong relationship between the predicted and response variables. The predicted latitude/longitude values are close enough to the reference latitude/longitude values as the points cluster around the trend line.

Model	MSE	$R^2$	MAE
ANFIS	0.000069	0.995479	0.000375
LSTM	0.010070	0.250617	0.006071
ELM	0.001746	0.931812	0.002186

**Table 7.**

Summary of the evaluation metrics for the selected best models for GPS latitude correction.



Model	MSE	R <sup>2</sup>	MAE
ANFIS	0.00005	0.997675	0.000042
LSTM	0.022376	0.110682	0.001096
ELM	0.004519	0.855484	0.000425

**Table 8.** Summary of the evaluation metrics for the selected best models for GPS longitude correction.

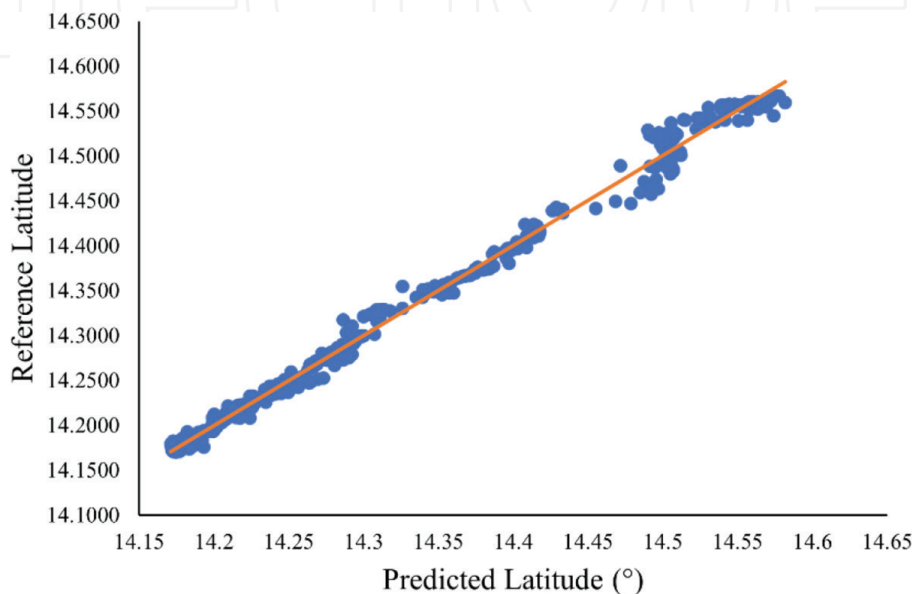


**Figure 11.** The resulting scatter plot of the predicted corrected latitude of the selected most superior ANFIS model versus the reference latitude data.

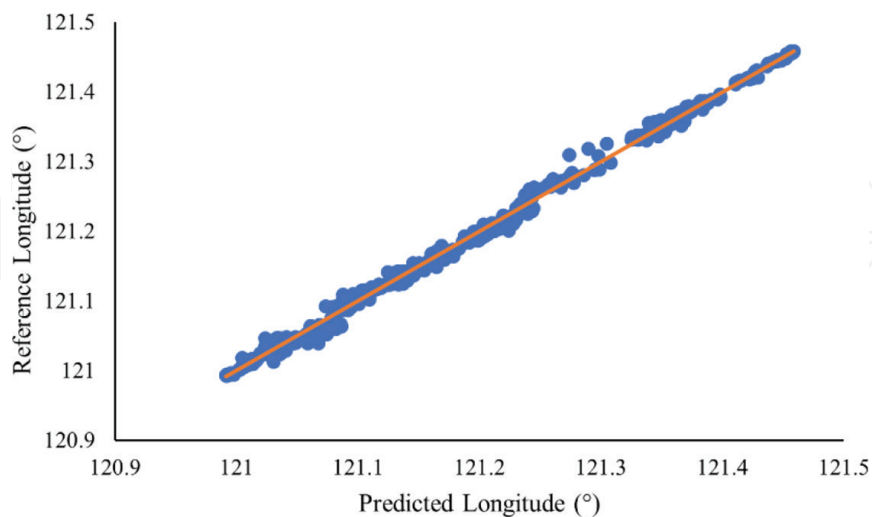


**Figure 12.** The resulting scatter plot of the predicted corrected longitude of the selected most superior ANFIS model versus the reference longitude data.

Therefore, the simulated ANFIS models still outperformed the LSTM and ELM models, which proved that these models can combine the advantageous features of neural networks and fuzzy logic in one framework. In giving better accuracy in

predicting the corrected latitude and longitude. The comparison of results also proved that ANFIS is a promising method for localization and tracking vehicles utilizing GPS and IMU data. In terms of generalization, ANFIS has demonstrated high generalization capability, which increases its robustness and accuracy when transforming fuzzy sets into crisp inputs [22].

### 3.4 Visualization results of the actual collected dataset by applying the selected best ANFIS models

To confirm the robustness of the selected best models, 2521 collected actual GPS-IMU datasets obtained from the conducted testing from Lumban, Laguna to DLSU, without the need of splitting the data, were used to test and visualize the ANFIS model performances. These actual datasets consist of the uncorrected GPS latitude and longitude coordinates. On the other hand, the corrected GPS latitude and longitude were predicted using the selected highest-performing ANFIS models (ANFIS model 1B for latitude and model 2B for longitude). The visualized map of the plotted actual GPS latitude and longitude dataset and the predicted corrected GPS latitude and longitude through ANFIS are presented in **Figure 13**. It shows that the uncorrected set of GPS latitude and longitude was too outlying and very distant from the predicted corrected output values generated by the ANFIS models. This signifies that the selected ANFIS models have the best performances to predict the correct GPS latitude and longitude.

The response of the predicted corrected GPS coordinates using the selected ANFIS models concerning the reference route and collected actual GPS coordinates are shown (**Figure 14**). The result of the plotted corrected GPS latitude and longitude coordinates (in green dotted line) is almost near the reference GPS coordinates (in blue line) compared to the collected actual GPS latitude and longitude (in red pin markers). According to the results, the proposed ANFIS models, that is, the fuzzy system combined with neural network capabilities, achieved better error reduction without the need to identify the system's noise type, as it was trained on the

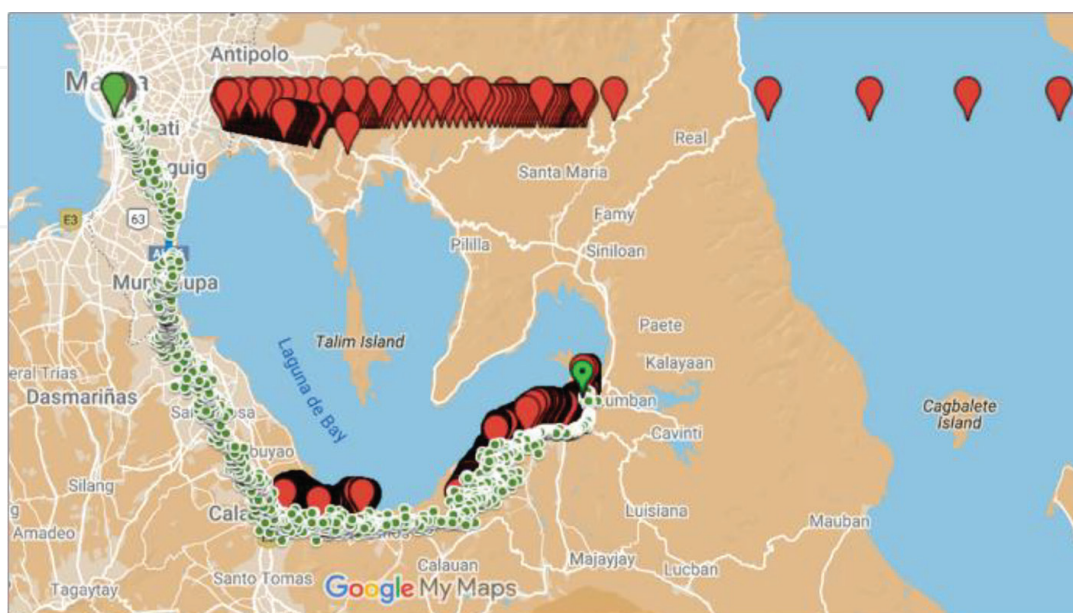


**Figure 13.** Visualization maps of the uncorrected GPS coordinates (red pin marker) versus the predicted corrected GPS coordinates (green dots).

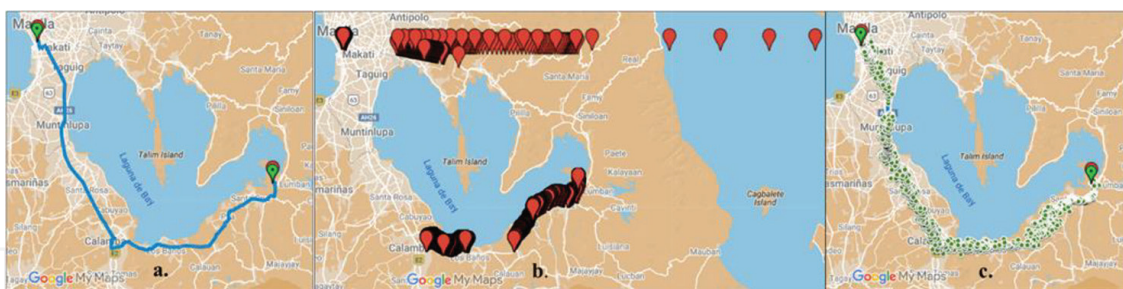


**Figure 14.** Resulting visualization maps for comparison of the (a) reference GPS coordinates, (b) uncorrected GPS coordinates, and (c) corrected GPS coordinates using the ANFIS models.

data region. This makes it a more convenient and cost-effective option than other state-of-the-art approaches. In the given noisy collected actual dataset, the selected ANFIS models have been proven to address the challenging and nonlinear problems while minimizing complexity in computation [27]. Because ANFIS models may be implemented in real-time, they are well suited for applications that demand rapid and precise data processing, particularly suitable for the localization and tracking of vehicle position [27]. Integrating the ANFIS models into the capacitive resistivity underground imaging towed antenna system can offer great significance in mapping the precise location of the surveyed underground utility objects.

However, verifying further the ANFIS models' performance requires the recollection of new GPS latitude and longitude datasets and testing this new data to the simulated ANFIS models. This is considered as the lacking approach of this study that can be done for future research. Additionally, to maximize the ANFIS model performance, it suggests retraining and adjusting the hyperparameters when tested in newly collected actual data. Also, the study's results can be further evaluated by comparing them with other methods of sensor fusion such as the use of other machine learning models which will be the next direction of the paper.

#### 4. Conclusion

The CR method utilizes GPS to create accurate maps quickly and with less equipment and labor than traditional surveying. However, errors can occur due to GPS sensor accuracy, digital map quality, and map-matching errors. To improve accuracy, an IMU-GPS sensor fusion method can be used. Environmental factors can still cause GPS sensors to fail, so reducing errors in GPS receiver accuracy is crucial for correct underground utility location and map matching. The study proposes using fuzzy logic with ANFIS to correct the latitude and longitude of the CR vehicle's position by integrating RTK-GPS sensor data with IMU linear acceleration and magnetometer data. The ANFIS tool trains two fuzzy systems, one for latitude and one for longitude correction. The developed combined GPS-IMU circuit was tested by conducting field testing from Lumban to De La Salle University Manila Campus to collect actual GPS latitude and longitude, triaxial accelerometer, and triaxial magnetometer data. The study evaluated different ANFIS models with varying hyperparameters, and the selected model for latitude correction is model 1B with a hybrid optimization algorithm at 300 training epochs. This model achieved the lowest training RMSE of 0.008770, validation RMSE of 0.008300, and testing RMSE of 0.011814 at 300 training epochs. Model 1B showed the lowest MSE of 0.000069, highest  $R^2$  of 0.995479, and lowest MAE of

0.000375 compared to other models, proving superior results. For ANFIS longitude correction, model 2B was selected, and a hybrid optimization algorithm was applied at 100 epochs, which resulted in the lowest training RMSE of 0.007361, 0.007100 validation RMSE, and 0.01532 testing RMSE. Among the four prediction models of model 2, model 2A achieved the lowest MSE of 0.000050, the highest  $R^2$  of 0.997675, and the lowest MAE of 0.000042 for longitude correction, demonstrating the best results.

The selected best ANFIS models' performances were then validated by comparing them to simulated LSTM and ELM models; however, the ANFIS models still outperformed the two other models. The ANFIS models were also tested on the collected actual dataset for verification of results. The visualized map obtained from this simulation test revealed that the uncorrected GPS data points were significantly distant from the target GPS reference values compared to the ANFIS corrected output. This indicates that the ANFIS models proved to combine the benefits of neural networks with fuzzy logic in a single structure for predicting corrected latitude and longitude with greater accuracy. The comparison of findings also demonstrated that ANFIS is a potential solution for vehicle localization and tracking using GPS and IMU data, making it suitable to be integrated into capacitive resistivity underground imaging system and can be extremely useful in mapping the precise location of the investigated subterranean utility objects.

To further validate the ANFIS models' performance, additional GPS latitude and longitude datasets must be collected and tested against the simulated ANFIS models. This is considered the study's lacking strategy that can be done for future research. Furthermore, it suggests retraining and adjusting the hyperparameters when tested on newly obtained actual data to maximize the ANFIS model performance. Lastly, the study's results can be further examined by comparing them to other ways of sensor fusion, such as the employment of other machine learning models, which will be the paper's next goal.

## **Acknowledgements**

The authors would like to thank the Department of Science and Technology – Philippine Council for Industry, Energy and Emerging Technology Research and Development (DOST-PCIEERD) and the Intelligent Systems Laboratory of the De La Salle University for all the granted support.

IntechOpen

### **Author details**

Elmer Dadios<sup>1,2\*</sup>, Jonah Jahara Baun<sup>2,3</sup>, Mike Louie Enriquez<sup>1,2</sup>,  
Adrian Genevie Janairo<sup>2,3</sup>, Ronnie Concepcion II<sup>1,2</sup>, Joseph Aristotle De Leon<sup>1,2</sup>,  
Kate Francisco<sup>1,2</sup>, Andres Philip Mayol<sup>2,4</sup>, Argel Bandala<sup>2,3</sup> and Ryan Rhay Vicerra<sup>1,2</sup>

1 Department of Manufacturing Engineering and Management, De La Salle University, Manila, Philippines

2 Center for Engineering and Sustainability Development Research, De La Salle University, Manila, Philippines


3 Department of Electronics and Computer Engineering, De La Salle University, Manila, Philippines

4 Department of Mechanical Engineering, De La Salle University, Manila, Philippines

\*Address all correspondence to: [elmer.dadios@dlsu.edu.ph](mailto:elmer.dadios@dlsu.edu.ph)

### **IntechOpen**

---

© 2023 The Author(s). Licensee IntechOpen. This chapter is distributed under the terms of the Creative Commons Attribution License (<http://creativecommons.org/licenses/by/3.0>), which permits unrestricted use, distribution, and reproduction in any medium, provided the original work is properly cited. 

## References

- [1] Ducut JD, Alipio M, Go PJ, Concepcion R II, Vicerra RR, Bandala A, et al. A review of electrical resistivity tomography applications in underground imaging and object detection. *Displays*. 2022;**73**:85-94
- [2] Suherman E, Wijayanto AH, Rambe N, Mubarakah YS, Al-Akaidi M. Underground object detection based on radio propagation characteristics. *Journal of Theoretical and Applied Information Technology*. 2021;**99**(1):63-71
- [3] Kuras O, Beamish D, Meldrum PI, Ogilvy RD. Fundamentals of the capacitive resistivity technique. *Geophysics*. 2006;**71**(3):29-41
- [4] Janairo AG, Baun JJ, Concepcion R, Relano R, Francisco K, Enriquez ML, et al. Optimization of subsurface imaging antenna capacitance through geometry modeling using Archimedes, Lichtenberg and Henry gas solubility metaheuristics. In: 2022 IEEE International IOT, Electronics and Mechatronics Conference (IEMTRONICS). Toronto, ON, Canada: Institute of Electrical and Electronics Engineers Inc.; 2022. pp. 1-8
- [5] Francisco K et al. Systematic analysis and proposed AI-based technique for attenuating inductive and capacitive parasitics in low and very low frequency antennas. In: IEEE International IOT, Electronics and Mechatronics Conference. Toronto, ON, Canada: Institute of Electrical and Electronics Engineers Inc.; 2022
- [6] Francisco K et al. Analytical hierarchical process-based material selection for trailer body frame of an underground imaging system. In: 2021 IEEE 13th International Conference on Humanoid, Nanotechnology, Information Technology, Communication and Control, Environment, and Management. Manila, Philippines: Institute of Electrical and Electronics Engineers Inc.; 2021
- [7] Baun JJ et al. Hybrid stochastic genetic evolution-based prediction model of received input voltage for underground imaging applications. In: 2023 8th International Conference on Business and Industrial Research (ICBIR). Bangkok, Thailand: IEEE; 2023. pp. 549-555. DOI: 10.1109/ICBIR57571.2023.10147464
- [8] Lo Monte L, Erricolo D, Soldovieri F, Wicks MC. Underground imaging of irregular terrains using RF tomography. In: 2009 3rd IEEE International Workshop on Computational Advances in Multi-Sensor Adaptive Processing (CAMSAP). Aruba, Netherland Antille: IEEE; 2009. pp. 229-232
- [9] Nandakumar N, Alex TK, Ajayakumar K, Rao KS. Capacitive resistivity imaging: Overview, modeling and applications. *Journal of Selected Topics in Applied Earth Observations and Remote Sensing (IEEE)*. Sep 2010;**3**(3):376-390
- [10] Hsu PC, Nurrachman MA. GPS limitations and solutions. In: 2019 IEEE International Conference on Systems, Man and Cybernetics (SMC). Bari, Italy: IEEE; 2019. pp. 2355-2360
- [11] Li J, Li Y, Li B, Yang D. Performance analysis and improvement of GPS positioning accuracy. *IEEE Access*. 2021;**9**:36368-36380
- [12] Islam MS, Rahman MH, Rashid MA, Khan MFR. Challenges and limitations of GPS: A review. In: 2017 International

Conference on Electrical, Computer and Communication Engineering (ECCE). Cox's Bazar, Bangladesh: IEEE; 2017. pp. 548-552. DOI: 10.1109/ECCE.2017.8307247

[13] Panda SS, Padhy PK. Map-matching algorithms for vehicle navigation: A survey. *Journal of Intelligent Transportation Systems*. 2014;**18**(2):99-117. DOI: 10.1080/15472450.2013.841344

[14] Zhou Y, Li H, Ding L. IMU/GPS fusion with extended Kalman filter for autonomous vehicle navigation. In: 2017 IEEE International Conference on Mechatronics and Automation (ICMA). Takamatsu: IEEE; 2017. pp. 648-653. DOI: 10.1109/ICMA.2017.8015795

[15] Shien C, Huang C, Liu J, Chen X, Weijinya U, Shi G. Integrated navigation accuracy improvement algorithm based on multi-sensor fusion. In: 2019 IEEE The 2nd International Conference on Micro/Nano Sensors for AI, Healthcare, and Robotics (NSENS). Shenzhen, China: IEEE; 2019. pp. 54-57. DOI: 10.1109/NSENS49395.2019.9293950

[16] Farhad M, Mosavi M, Abedi A, Mohammadi K. Increasing the resistance of GPS receivers by using a fuzzy smart estimator in weak signal conditions. *The Journal of Navigation*. 2020;**73**(5):991-1013. DOI: 10.1017/S0373463320000132

[17] Correa-Caicedo PJ, Barranco-Gutiérrez AI, Guerra-Hernandez EI, Batres-Mendoza P, Padilla-Medina JA, Rostro-González H. An FPGA-based architecture for a latitude and longitude correction in autonomous navigation tasks. *Measurement*. 2021;**182**:109757. DOI: 10.1016/j.measurement.2021.109757

[18] Kathpalia N, Gulati T. Enhancement of GPS accuracy using combination of active antenna ground plane enhancement, sensor fusion compressing

3 axis gyro accelerometer & artificial intelligence. *Mathematical Statistician and Engineering Applications*. 2022;**71**(3s2):2067-2083

[19] Tehrani M, Nariman-Zadeh N, Masoumnezhad M. Adaptive fuzzy hybrid unscented/H-infinity filter for state estimation of nonlinear dynamics problems. *Transactions of the Institute of Measurement and Control*. 2019;**41**(6):1676-1685

[20] Woo R, Yang E-J, Seo D-W. A fuzzy-innovation-based adaptive Kalman filter for enhanced vehicle positioning in dense urban environments. *Sensors*. 2019;**19**(5):1142. DOI: 10.3390/s19051142

[21] Zhu J, Tang Y, Shao X, Xie Y. Multisensor fusion using fuzzy inference system for a visual-IMU-wheel odometry. *IEEE Transactions on Instrumentation and Measurement*. 2021;**70**:2505216. DOI: 10.1109/TIM.2021.3105867

[22] Chopra S, Dhiman G, Sharma A, Shabaz M, Shukla P, Arora M. Taxonomy of adaptive neuro-fuzzy inference system in modern engineering sciences. *Computational Intelligence and Neuroscience*. 2021;**2021**:6455592. DOI: 10.1155/2021/6455592

[23] Sun R, Hsu L, Xue D, Zhang G, Ochieng W. GPS signal reception classification using adaptive neuro-fuzzy inference system. *The Journal of Navigation*. 2019;**72**(3):685-701. DOI: 10.1017/S0373463318000899

[24] Correa Caicedo P, Rostro-Gonzalez H, Rodriguez-Licea M, Gutiérrez-Frías Ó, Herrera-Ramírez C, Méndez-Gurrola I, et al. GPS data correction based on fuzzy logic for tracking land vehicles. *Mathematics*. 2021;**9**(21):2818. DOI: 10.3390/math9212818

[25] Duan Y, Li H, Wu S, Zhang K. INS error estimation based on an ANFIS and

its application in complex and covert surroundings. *ISPRS International Journal of Geo-Information*. 2021;**10**(6):399. DOI: 10.3390/ijgi10060388

[26] Ajani OS, El-Hussieny H. An ANFIS-based human activity recognition using IMU sensor fusion. In: 2019 Novel Intelligent and Leading Emerging Sciences Conference (NILES). Giza, Egypt: Institute of Electrical and Electronics Engineers Inc.; 2019. pp. 34-37. DOI: 10.1109/NILES.2019.8909289

[27] El Shafie A, Hussain A, Eldin AEN. ANFIS-based model for real-time INS/GPS data fusion for vehicular navigation system. In: 2009 International Conference on Computer Technology and Development. Kota Kinabalu, Malaysia: Institute of Electrical and Electronics Engineers Inc.; 2009. pp. 278-282. DOI: 10.1109/ICCTD.2009.42

[28] Hosseinyalamdary S. Deep Kalman filter: Simultaneous multi-sensor integration and modelling, a GNSS/IMU case study. *Sensors (Basel)*. 2018;**18**(5):1316. DOI: 10.3390/s18051316

[29] De Leon JA et al. Robotic simulation and GPS position estimation of a towed CRI equipment using Savitzky-Golay filter. In: IEEE Region 10 Annual International Conference, Proceedings/TENCON. Hong Kong, Hong Kong: Institute of Electrical and Electronics Engineers Inc.; 2022. DOI: 10.1109/TENCON55691.2022.9977685

[30] Stangebye T, Mohr T, Vallenti A, Grauff M, Koziol S. Custom real-time-kinematics positioning system testbed for mobile robot localization. In: Proc. of the IEEE Dallas Circuits and Systems Conference. Dallas, TX, USA: Institute of Electrical and Electronics Engineers Inc.; 2020. pp. 221-224. DOI: 10.1109/DCAS51144.2020.9330659

[31] Broekman A, Gräbe J. A low-cost, mobile real-time kinematic geolocation service for engineering and research applications specifications table. *HardwareX*. 2021;**10**:e00203. DOI: 10.17605/OSF.IO/QH3V7

[32] Abdelfatah R, Moawad A, Alshaer N, Ismail T. UAV tracking system using integrated sensor fusion with RTK-GPS. In: 2021 International Mobile, Intelligent, and Ubiquitous Computing Conference, MIUCC 2021. Cairo, Egypt: Institute of Electrical and Electronics Engineers Inc.; 2021. pp. 352-356. DOI: 10.1109/MIUCC52538.2021.9447646

[33] Brossard M, Barrau A, Bonnabel S. AI-IMU dead-reckoning. *IEEE Transactions on Intelligent Vehicles*. 2020;**5**(4):585-595. DOI: 10.1109/TIV.2020.2980758

[34] Fazeli H, Samadzadegan F, Dadrasjavan F. Evaluating the potential of RTK-UAV for automatic point cloud generation in 3D rapid mapping. In: International Archives of the Photogrammetry, Remote Sensing and Spatial Information Sciences - ISPRS Archives. Prague, Czech Republic: International Society for Photogrammetry and Remote Sensing; 2016. pp. 221-226. DOI: 10.5194/isprsarchives-XLI-B6-221-2016

[35] Lauguico S, Baldovino R, Concepcion R, Alejandrino J, Tobias RR, Dadios E. Adaptive neuro-fuzzy inference system on aquaphotomics development for aquaponic water nutrient assessments and analyses. In: ICITEE 2020 - Proceedings of the 12th International Conference on Information Technology and Electrical Engineering. Yogyakarta, Indonesia: Institute of Electrical and Electronics Engineers Inc.; 2020. pp. 317-322. DOI: 10.1109/ICITEE49829.2020.9271736



- [36] Jang JSR. ANFIS: Adaptive-network-based fuzzy inference system. *IEEE Transactions on Systems, Man and Cybernetics*. 1993;**23**(3):665-685. DOI: 10.1109/21.256541
- [37] Francisco KG, Relano RS, Concepcion RS, Enriquez ML, Vicerra RR, Baun JJ, et al. Adaptive neuro-fuzzy active spring control of a vibration isolator for towed capacitive resistivity imaging single trailer. In: 2022 IEEE 14th International Conference on Humanoid, Nanotechnology, Information Technology, Communication and Control, Environment, and Management (HNICEM). Boracay Island, Philippines: Institute of Electrical and Electronics Engineers Inc.; 2022. pp. 1-6. DOI: 10.1109/HNICEM57413.2022.10109420
- [38] Panoiu M, Panoiu C, Lihaciu IL. Adaptive neuro fuzzy system for modelling and prediction of distance pantograph catenary in railway transportation. *IOP Conference Series: Materials Science and Engineering*. 2018;**294**(1):1-7. DOI: 10.1088/1757-899X/294/1/012073
- [39] Arafah L, Singh H, Putatunda SK. A neuro fuzzy logic approach to material processing. *IEEE Transactions on Systems, Man, and Cybernetics Part C (Applications and Reviews)*. 1999;**29**(3):362-370. DOI: 10.1109/5326.777072
- [40] Prakash S, Jalal AS, Pathak P. Forecasting COVID-19 pandemic using prophet, LSTM, hybrid GRU-LSTM, CNN-LSTM, Bi-LSTM and stacked-LSTM for India. In: 2023 6th International Conference on Information Systems and Computer Networks (ISCON). Mathura, India: Institute of Electrical and Electronics Engineers Inc.; 2023. pp. 1-6. DOI: 10.1109/ISCON57294.2023.10112065
- [41] Vashisht S, Kumar P, Trivedi MC. Improvised extreme learning machine for crop yield prediction. In: 2022 3rd International Conference on Intelligent Engineering and Management (ICIEM). London, United Kingdom: Institute of Electrical and Electronics Engineers Inc.; 2022. pp. 754-757. DOI: 10.1109/ICIEM54221.2022.9853054
- [42] Sa'ad Kusri MI, Mustafa MS. Student prediction of drop out using extreme learning machine (ELM) algorithm. In: 2020 2nd International Conference on Cybernetics and Intelligent System (ICORIS). Manado, Indonesia: Institute of Electrical and Electronics Engineers Inc.; 2020. pp. 1-6. DOI: 10.1109/ICORIS50180.2020.9320831
- [43] Zhu QY, Qin AK, Suganthan PN, Huang GB. Evolutionary extreme learning machine. *Pattern Recognition*. 2005;**38**(10):1759-1763. DOI: 10.1016/j.patcog.2005.03.028